Canadian Mineralogist
Vol. 28, pp. 267-285 (1990)

THE DELORO ANOROGENIC IGNEOUS COMPLEX, MADOC, ONTARIO. II. EVOLUTION AND POST-ERUPTION METASOMATISM OF THE VOLCANIC UNITS†

ABDEL-FATTAH M. ABDEL-RAHMAN* AND ROBERT F. MARTIN
Department of Geological Sciences and Mineral Exploration Research Institute,
McGill University, 3450 University Street, Montreal, Quebec H3A 2A7

ABSTRACT

The epizonal Deloro anorogenic igneous complex, located near Madoc, Ontario, of middle Proterozoic age, is associated with a suite of mafic and felsic volcanic rocks. These rocks are petrographically and geochemically distinct from rocks of the Tudor suite, to which they had been assigned. Where relatively unmetasomatized, trachyte and rhyolite show affinities to the syenite - hypersolvus granite - granophyre suite. In many cases, however, the rocks have undergone extensive postmagmatic alkali exchange, leading to extremely Na-rich or K-rich compositions; the metasomatic overprint has affected the concentration of some high-field-strength elements such as Y, as well as the rare earths. Although some of the textural features indicative of a volcanic origin have survived the metasomatic overprint and the later metamorphic overprint, the mineralogy of the suite, and in particular that of the feldspars, has been reset at a low subsolidus temperature (<200°C), and more completely so than in the plutonic members of the suite. Widespread Na-metasomatism of the volcanic suite seems to have been followed by more localized K-metasomatism at a lower temperature.

Keywords: Deloro anorogenic complex, Grenville Province, basalt, trachyte, rhyolite, alkali exchange, metasomatism, microcline, Ontario.

SOMMAIRE

Le complexe igné anorogénique épizonal de Deloro, situé près de Madoc, en Ontario, d'âge protérozoïque moyen, possède un cortège de roches volcaniques mafiques et felsiques. Ces roches se distinguent, aussi bien pétrographiquement que géochimiquement, des roches de la suite de Tudor, avec laquelle elles avaient été identifiées. Les échantillons les moins touchés par une métasomatose montrent des traits communs avec la suite plutonique syénite - granite hypersolvus - granophyre. Toutefois, dans plusieurs cas, les roches volcaniques ont été profondément affectées par un échange d'alcalins à un stade post-magmatique, ce qui a mené à des compositions extrêmement sodiques ou potassiques. La réaction a même causé une remobilisation de certains éléments à rapport élevé de valence à rayon ionique, par exemple Y, ainsi que des terres rares. Quoique certaines textures indicatives d'une origine volcanique ont survécu l'événement métasomatique et un épisode de métamorphisme régional, les assemblages minéralogiques, et en particulier les feldspaths, ont ré-équilibré à une température inférieure à 200°C, et de façon plus efficace que dans les membres plutoniques du complexe. Le flux hydrothermal à haute température, plus répandu, a d'abord effectué une métasomatose sodique, et ensuite, à plus basse température et dans un volume de roche beaucoup plus restreint, une métasomatose potassique.

Mots-clés: complexe anorogénique de Deloro, province du Grenville, basalte, trachyte, rhyolite, échange d'alcalins, métasomatose, microcline, Ontario.

INTRODUCTION

The suggestion was made, in our paper on the middle Proterozoic Deloro anorogenic gabbro - syenite - granite complex, in the Madoc area of southeastern Ontario (Abdel-Rahman & Martin 1987), that the extrusive rocks found immediately east of the granitic core of the complex [the so-called "Madoc Volcanics" of Hewitt (1968), a term that should be abandoned, according to Easton (1989a)], constitute part of its volcanic cover. Bartlett *et al.* (1984) had earlier raised this possibility. The suggestion was made for three reasons: 1) the volcanic rocks occur inside a subcircular structure (Fig. 1A); 2) the rocks are petrographically distinct from, and considerably less deformed than, those assigned to the Tudor Formation (Hermon Group), usually considered the base of the Grenville Supergroup in southeastern Ontario, and 3) felsic rock-types are more abundant than in the Tudor suite. In spite of these distinguishing features, Hewitt (1968) had assigned all the volcanic rocks in the Madoc area to the Tudor Formation. Most other investigators have accepted this assignment (*e.g.*, Moore & Thompson 1980). Easton (1989b) has questioned whether these fine-grained rocks are perhaps not simply contact-metasomatized metasedimentary and meta-igneous rocks.

In this paper, we focus on the volcanic members of the Deloro complex, *i.e.*, the "Madoc Volcanics" of Hewitt (1968). In terms of bulk composition, some felsic rocks seem to be undisturbed, and as such closely related to the plutonic members of the Deloro

---

*Present address: Department of Geology, Concordia University, 7141 Sherbrooke Street West, Montreal, Quebec H4B 1R6.

†Mineral Exploration Research Institute publication number A9013.

complex. Other felsic samples have undergone an exchange of alkalis. The same process has affected part of the mafic volcanic unit. The pattern of metasomatic adjustments within the Deloro volcanic suite is typical of that found in classic examples of anorogenic epizonal complexes. In this paper, our objectives are 1) to provide geochemical and mineralogical information to characterize this volcanic suite, 2) to propose an interpretation of the petrogenesis of those rocks whose chemical composition is still close to being primary, and 3) to discuss the distribution of post-eruption metasomatism and its effect on the selective mobility of major and trace elements.

The Geological Context

A generalized geological map of the Deloro complex (Fig. 1A) illustrates the distribution of the plutonic rocks, volcanic rocks, and a folded septum of metasedimentary rocks that are assigned to the Flinton Group (Moore & Thompson 1980) [this assignment has been questioned by Easton (1989a)]. These middle Proterozoic rocks are partly concealed by flat-lying Ordovician limestone. Hewitt (1968) mapped two distinct units of volcanic rocks, referred to as andesitic and rhyolitic [the symbols M (for mafic) and F (for felsic) are used in Figs. 1A, B]. Outcrops cover roughly 30% of the area labeled M and F; the best exposures occur along highways 7 and 62 (Fig. 1B).

The "andesitic" or mafic rocks are massive, greenish grey to black, generally nonporphyritic and only locally deformed. Inclusions of marble typically range from 2 to 40 cm across, and are common. The unit is mapped as being unconformably overlain by rocks of the Flinton Group (Moore & Thompson 1980, Fig. 5). The Flinton Group has been considered younger than the Deloro pluton even though it is more intensely deformed and is metamorphosed to a higher grade (upper greenschist to lower amphibolite facies; the rocks are locally kyanite-bearing) than the Deloro igneous suite. The petrofabric and radiometric analyses of Connelly *et al.* (1987) east of the Elzevir batholith, 25 km northeast of Madoc, raise the possibilities that 1) the Flinton Group is in fact

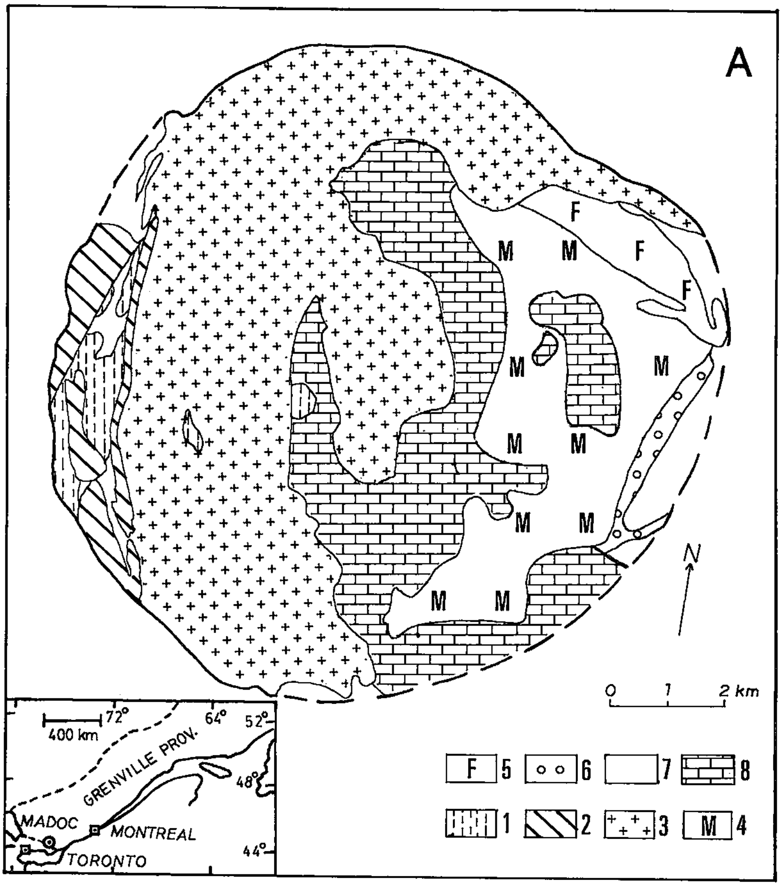

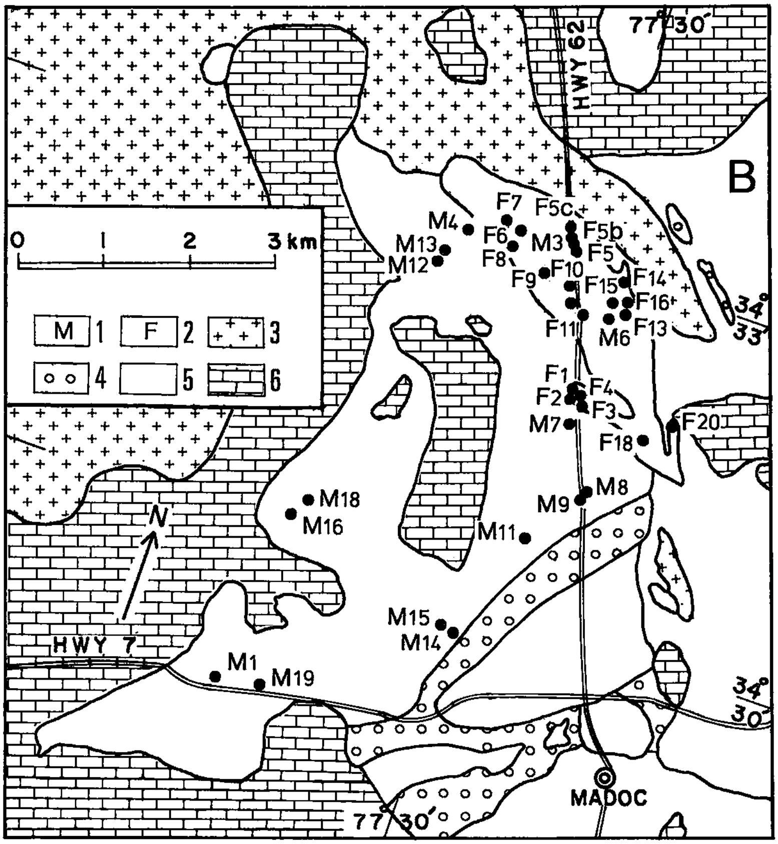

FIG. 1. A. Generalized geological map of the Deloro complex, southeastern Ontario, showing the relationship of the volcanic units (labeled M and F) to the plutonic members of the inferred ring-complex. The map is based on those of Hewitt (1968) and Bartlett & Moore (1983). Symbols: 1 gabbro, 2 syenite, 3 peralkaline granite and granophyre, 4 mafic volcanic suite, 5 felsic volcanic suite, 6 metaconglomerate and pelitic schist (Skootamatta and Madoc Formations), 7 (inside the inferred ring-fault) marble (Stewart Formation), 8 Ordovician limestone. Units 1-7 are middle Proterozoic in age. B. Sample-location map showing the distribution of samples of the mafic (1) and felsic (2) units. Other symbols: 3 felsic plutonic members of the complex; 4, 5 and 6 correspond to 6, 7 and 8, respectively, in Figure 1A.

older than the Elzevir batholith (1229^{+11}_{-4} Ma) and, by extension, perhaps the Deloro complex (1241 ± 2 Ma: van Breemen & Davidson 1989) as well, and 2) the contact between the volcanic unit and the Flinton is intrusive or tectonic.

The felsic volcanic rocks occupy a more restricted area than do the more mafic rocks (Figs. 1A, B). The felsic units vary from pink to black, and generally are nonporphyritic and massive. They commonly enclose irregularly shaped blobs of mafic material from 5 to 20 cm across; the presence of mottled pink-and-black rocks and the widespread occurrence of an intimate mixture of the two rock types, as illustrated by Hewitt's (1968) use of the labels "2b - 1a" and "1a - 2b" (2b: massive "andesite", 1a: rhyolite tuff) to define the map-units, suggest that the two magmas coexisted.

The felsic plutonic members of the Deloro complex have attracted considerable attention [*cf.* Abdel-Rahman & Martin (1987) and references therein]. Tuttle (1952) and Tuttle & Bowen (1958) used the Deloro granite to define the type hypersolvus granite. It is a typical peralkaline A-type granite indicative of an anorogenic, within-plate tectonic setting at the time of emplacement, 1241 Ma ago. Precious-metal and base-metal mineralization is associated with the pluton (Sangster & Bourne 1982, Malczak *et al.* 1985). In contrast, the associated volcanic rocks have barely been mentioned in the literature, presumably because of Hewitt's assignment to a regionally widespread map-unit.

PETROGRAPHY

The volcanic suite contains virtually unmodified as well as compositionally modified varieties. Most of these rocks still preserve textures typical of volcanic igneous rocks, though the textures are modified by recrystallization and metasomatism. Signs of penetrative deformation are encountered only rarely.

The mafic volcanic unit (M, Figs. 1A, B, Appendix 1) consists mainly of basalt and trachyandesite.

TABLE 1. CHEMICAL COMPOSITION OF REPRESENTATIVE SAMPLES OF THE VOLCANIC UNITS*

	M1	M3	M4	M6	M7	M8	M9	M11	M12	M13	M14	M15	M16	M18	M19	T1	T2	T3	F1	F2
SiO_2	62.08	54.71	61.91	47.74	58.86	51.02	49.64	59.11	59.52	55.20	49.53	50.69	67.68	66.41	59.44	49.71	49.15	50.00	68.87	67.54
TiO_2	0.53	1.69	0.95	2.52	1.37	2.21	2.45	1.39	1.43	1.60	2.07	2.14	0.56	0.53	1.15	0.80	0.35	0.51	0.44	0.49
Al_2O_3	11.92	16.10	16.19	13.35	13.98	15.05	14.76	13.93	13.96	15.46	13.86	13.85	12.96	11.90	13.78	19.37	21.17	20.95	14.42	13.60
Fe_2O_3	2.83	3.07	2.32	5.00	3.05	3.76	4.28	2.98	3.07	2.75	3.34	3.59	2.38	2.70	3.68	2.91	2.70	2.25	0.47	0.88
FeO	7.67	8.33	6.28	13.58	8.28	10.21	11.62	8.09	8.32	7.45	9.06	9.75	6.44	7.34	9.97	7.91	7.31	6.12	1.28	2.37
MnO	0.44	0.03	0.02	0.06	0.23	0.19	0.21	0.15	0.15	0.03	0.18	0.24	0.06	0.09	0.16	0.16	0.12	0.15	0.01	0.03
MgO	1.08	2.52	2.42	4.33	1.20	4.96	5.25	1.58	1.69	0.99	2.83	4.35	0.42	0.95	1.15	5.05	5.66	5.56	0.32	0.26
CaO	3.32	2.74	1.32	3.84	5.15	8.09	7.26	3.88	3.90	4.87	9.07	8.46	0.59	1.35	1.33	9.16	7.79	8.14	0.85	2.35
Na_2O	4.09	7.54	2.08	1.56	3.28	4.08	4.25	4.82	4.78	8.06	3.98	3.43	4.80	4.06	4.33	3.70	4.17	4.67	0.87	2.17
K_2O	3.53	1.77	4.98	5.16	2.39	0.24	0.49	1.76	1.76	1.04	0.19	0.68	3.82	3.10	3.76	0.92	1.47	0.41	11.02	8.04
P_2O_5	0.06	0.38	0.13	0.27	0.42	0.25	0.30	0.41	0.42	0.51	0.25	0.26	0.06	0.04	0.30	0.15	0.04	0.06	0.11	0.11
LOI	2.81	2.01	2.16	2.86	2.64	1.37	0.92	2.20	1.73	2.83	6.35	3.47	0.63	1.54	0.96	0.74	1.06	2.03	0.82	2.02
Total	100.40	100.95	100.82	100.35	100.91	101.47	101.48	100.35	100.77	100.81	100.74	100.97	100.44	100.05	100.06	100.60	101.03	100.89	99.57	99.92
Qtz	13.9	-	21.3	-	15.7	0.3	-	11.5	11.7	-	3.1	3.2	19.3	22.6	10.0	-	-	-	19.5	19.7
Or	21.4	10.6	29.8	31.3	14.4	1.4	2.9	10.6	10.5	6.3	1.2	4.1	22.6	18.6	22.4	5.4	8.7	2.5	66.0	48.6
Ab	35.5	55.2	17.9	13.6	28.3	34.5	35.8	41.6	40.9	57.4	35.7	29.8	40.7	34.9	37.0	31.4	27.5	36.4	7.5	18.8
An	3.8	4.9	5.8	14.6	16.7	22.0	19.7	11.4	11.6	3.0	20.6	20.9	40.7	5.2	4.7	33.6	34.7	35.4	2.9	3.7
DI	70.8	65.8	69.0	44.9	58.4	36.2	38.7	63.7	63.1	63.7	40.0	37.1	82.6	76.1	69.4	36.8	36.2	38.9	93.0	87.1
A/CNK	0.72	0.83	1.44	0.88	0.81	0.69	0.71	0.82	0.83	0.67	0.60	0.64	0.99	0.95	1.01	0.82	0.94	0.91	0.97	0.82
NK/A	0.89	0.89	0.55	0.61	0.57	0.46	0.51	0.71	0.70	0.93	0.49	0.46	0.93	0.84	0.81	0.37	0.40	0.39	0.93	0.90
K/NK	0.36	0.13	0.61	0.69	0.32	0.04	0.07	0.19	0.19	0.08	0.03	0.11	0.34	0.33	0.36	0.14	0.19	0.06	0.89	0.71

	F3	F4	F5	F5b	F5c	F6	F7	F8	F9	F10	F11	F12	F13	F14	F15	F16	F18	F20	F23	F24
SiO_2	64.08	57.21	77.81	77.21	72.53	75.62	76.03	61.24	76.01	61.55	61.12	64.37	72.00	62.68	75.27	64.53	65.08	59.99	79.24	72.15
TiO_2	0.81	1.27	0.11	0.05	0.15	0.21	0.17	1.21	0.16	0.93	0.98	1.27	0.18	1.08	0.13	1.01	0.69	0.74	0.10	0.26
Al_2O_3	15.95	17.93	13.33	13.43	12.69	14.33	13.61	18.19	13.38	14.34	15.22	15.81	13.81	17.76	12.94	16.16	13.16	16.29	11.93	14.90
Fe_2O_3	1.49	1.77	0.13	0.12	0.36	0.19	0.22	0.77	0.19	1.69	2.42	0.79	0.25	0.97	0.15	0.52	1.40	0.53	0.16	0.61
FeO	4.05	4.80	0.34	0.34	0.97	0.51	0.60	2.08	0.50	4.58	6.55	2.13	0.68	2.64	0.41	1.41	3.81	1.45	0.45	1.84
MnO	0.02	0.03	0.01	0.01	0.02	0.02	0.03	0.02	0.01	0.04	0.02	0.01	0.02	0.04	0.02	0.05	0.01	0.08	0.01	0.02
MgO	0.71	0.87	0.18	0.30	1.48	0.06	0.00	0.12	0.43	0.40	0.35	0.20	0.20	0.67	0.01	0.31	0.14	0.88	0.25	0.93
CaO	1.50	2.40	0.20	0.34	2.27	0.29	0.42	3.27	0.50	3.85	2.05	1.07	0.39	1.79	0.05	3.74	0.96	2.78	0.52	1.16
Na_2O	4.66	4.67	7.44	7.58	6.22	8.22	7.98	7.09	7.59	4.95	5.13	1.10	1.44	8.71	1.47	7.56	0.60	0.98	6.62	0.01
K_2O	5.19	7.21	0.37	0.25	1.22	0.31	0.27	4.38	0.41	5.06	4.60	11.68	9.84	1.66	9.11	1.51	10.70	12.85	0.41	5.84
P_2O_5	0.15	0.23	0.02	0.02	0.03	0.03	0.02	0.23	0.01	0.22	0.23	0.21	0.02	0.20	0.02	0.19	0.16	0.24	0.02	0.05
LOI	1.56	2.10	0.34	0.41	2.12	0.46	0.71	1.70	0.74	2.96	1.74	1.13	0.61	2.01	0.35	2.93	3.28	3.06	0.58	2.50
Total	100.26	100.69	100.28	100.06	100.10	100.26	100.05	100.37	99.96	100.63	100.49	99.87	99.55	100.28	100.03	99.94	100.09	100.01	100.29	100.22
Qtz	11.2	-	32.3	30.9	26.4	25.8	27.9	-	28.9	6.2	6.5	10.9	24.8	1.0	31.7	9.4	17.7	0.2	37.8	45.9
Or	31.1	43.3	2.2	1.5	7.4	1.8	1.6	26.3	2.4	30.6	27.4	70.0	58.8	10.0	54.1	9.2	65.4	78.4	2.4	35.5
Ab	40.0	32.4	63.0	64.4	53.7	69.7	68.0	57.0	64.7	42.9	44.0	9.4	12.3	75.1	12.5	66.0	5.3	8.6	56.2	0.1
An	6.6	6.8	0.9	1.6	3.2	1.2	0.5	4.9	1.2	2.0	5.0	3.8	1.8	4.5	0.1	5.9	1.7	2.2	1.6	5.6
DI	82.3	75.7	97.5	96.8	87.5	97.3	97.5	83.3	96.0	79.7	78.1	90.3	95.9	86.1	98.3	84.6	88.4	87.2	96.4	81.5
A/CNK	1.00	0.90	1.02	1.00	0.81	1.00	0.96	0.81	0.97	0.70	0.89	0.97	1.01	0.92	1.05	0.77	0.92	0.79	0.97	1.77
NK/A	0.83	0.86	0.95	0.95	0.91	0.97	0.99	0.90	0.97	0.95	0.88	0.91	0.94	0.91	0.95	0.87	0.95	0.95	0.95	0.43
K/NK	0.42	0.50	0.03	0.02	0.11	0.02	0.02	0.29	0.04	0.40	0.37	0.88	0.82	0.11	0.80	0.12	0.92	0.90	0.04	1.00

* Also shown is the composition of three representative samples of basic volcanic rocks from the Tudor Formation (T1, T2 and T3). These were sampled 12 km northeast of the Deloro pluton, northeast of Queensborough. The data were obtained by standard XRF analysis; Fe^{2+} was determined by titration. Abbreviations: DI: differentiation index, the sum of normative Qtz, Ab and Or (Thornton & Tuttle 1960); A/CNK: $Al_2O_3/(CaO + Na_2O + K_2O)$; NK/A: $(Na_2O + K_2O)/Al_2O_3$, also known as the agpaitic index; K/NK: $K_2O/(Na_2O + K_2O)$. The last three indices are calculated using molar values; the normative constituents are expressed in weight %. The location of samples taken from units M and F is shown in Figure 1B; not shown there are F23 and F24; they are equivalent to 4-1 and the mineralized vein-material, respectively, studied by Abdel-Rahman & Martin (1987, Fig. 1, Tables 4, 5). Concentrations in wt.%.

The basalt contains irregularly oriented and glomeroporphyritic prisms of actinolitic amphibole (bluish green), plagioclase laths, chlorite and opaque phases in a microcrystalline groundmass. In amygdaloidal varieties, the amygdules are lined with relatively coarse quartz, chlorite and muscovite, and filled mostly with carbonate. Skeletal aggregates of chlorite and opaque phases may represent former pyroxene phenocrysts. Among the samples of trachyandesite, both aphyric and porphyritic varieties are present. The rock contains chloritized actinolitic amphibole, biotite, sericitized plagioclase and opaque phases in a microcrystalline groundmass. The presence of actinolitic amphibole, chlorite, albite (see below) and calcite suggests a metamorphic overprint in the greenschist facies.

The felsic volcanic suite occupies a small area labeled F in Figures 1A and 1B, and comprises trachytic and rhyolitic varieties. Aphyric and porphyritic rocks both are present; phenocrysts make up between 5 and 20% of the porphyritic varieties. Aphyric trachyte is composed of roughly aligned feldspar laths (*i.e.*, a trachytic texture) indicative of flow (*e.g.*, F8, F20, M13 in Appendix 1) embedded in a microcrystalline to cryptocrystalline groundmass mostly of anhedral feldspar, quartz and opaque phases. Phenocrysts in porphyritic trachyte consist of albite or K-feldspar (see below); the groundmass contains quartz, feldspar, biotite, chlorite and opaque minerals (including pyrite), is microcrystalline to cryptocrystalline, and is attributed an origin by devitrification. Most phenocrysts exhibit a very irregular outline, indicative of overgrowth, either into a largely molten groundmass or during metasomatism. A glomeroporphyritic texture characterizes both porphyritic trachyte and rhyolite. Aggregates of grid-twinned microcline (*e.g.*, F7, F15) are associated with secondary calcite. Devitrified volcanic clasts also are present.

Aphyric rhyolite consists of a cryptocrystalline mosaic of anhedral feldspar and quartz, which locally define a spherulitic texture (*e.g.*, F5a, F5b). Porphyritic rhyolite contains phenocrysts of inverted β-quartz and feldspar, with biotite, secondary muscovite, chlorite and opaque phases; the groundmass is a cryptocrystalline mosaic of quartz and albite or K-feldspar (or both). Some samples (*e.g.*, F15) show hematite-stained recrystallized flow-bands rich in secondary quartz and microcline, which alternate with finer grey cryptocrystalline bands. Albite or twinned microcline, along with muscovite, line cavities.

In general, the felsic rocks show evidence of flow-related textures; although volcanic fragments locally are present, the rocks are not considered tuffaceous, and thus do not seem to have been emplaced explosively. As pointed out above, Hewitt (1968) had concluded otherwise.

TABLE 2. CONCENTRATION OF SELECTED TRACE ELEMENTS IN SAMPLES OF THE VOLCANIC UNITS*

ppm	M1	M3	M4	M6	M7	M8	M9	M11	M12	M13	M14	M15	M16	M18	M19	T1	T2	T3	F1	F2
Rb	63	54	164	256	39	7	14	39	47	47	8	18	122	124	87	28	36	13	204	147
Ba	288	430	482	497	640	nd	139	510	509	137	nd	223	436	337	673	135	100	182	890	613
Sr	42	176	122	107	138	226	243	210	4	228	137	310	32	29	69	247	227	265	94	118
Zr	1123	279	217	183	349	168	184	352	788	261	163	171	1533	1309	504	91	60	80	255	209
Nb	36	20	17	16	27	19	20	27	36	18	19	20	47	38	29	18	15	17	18	19
Y	194	45	22	37	88	44	53	85	130	62	39	44	193	119	95	21	7	15	16	30

ppm	F3	F4	F5	F5b	F5c	F6	F7	F8	F9	F10	F11	F12	F13	F14	F15	F16	F18	F20	F23	F24
Rb	156	163	75	86	165	51	45	143	41	105	171	79	137	123	84	192	74	120	64	145
Ba	827	1171	nd	24	194	107	nd	581	115	661	730	831	1182	235	1372	167	950	1070	nd	574
Sr	156	163	75	86	165	51	45	143	41	105	171	79	137	123	84	192	74	120	64	145
Zr	376	203	187	109	199	333	306	247	299	727	309	191	313	227	392	212	119	352	187	197
Nb	20	16	15	14	9	26	25	20	26	41	19	16	25	14	23	11	14	19	13	4
Y	41	31	19	16	19	91	94	20	91	184	42	40	51	37	67	20	9	33	19	53

ppm	M6	M13	M18	F3	F5	F8	F11	F12	F15	F16	F20
Hf	5	8	36	12	6	6	9	5	15	5	9
La	14	22	77	25	13	8.4	23	13	36	11	18
Ce	30	51	165	54	24	18	49	26	68	21	37
Nd	21	36	93	35	12	13	31	17	33	11	19
Sm	6.4	11	24	9	2.8	3.6	8.3	5.3	8.9	2.9	4.8
Eu	1.8	3.3	3.5	2.1	0.6	1.0	2.4	1.7	1.0	1.0	1.1
Ho	2.0	2.7	6.8	2.1	1.2	1.1	2.1	nd	4.0	nd	1.5
Yb	4.4	6.0	19	5.9	3.3	3.0	5.4	3.2	12	2.2	3.9
Lu	0.6	1.0	2.8	0.9	0.5	0.5	0.8	0.5	1.8	0.3	0.6

* Also shown are data for three samples of basic volcanic rocks from the Tudor Formation (T1, T2, and T3). These data were obtained by standard techniques of XRF analysis (Rb, Ba, Sr, Zr, Nb and Y), and neutron-activation analysis (Hf and the rare earths). nd: concentration is below detection limits. For the purpose of drawing Figure 8B, F12 and F16 are assigned concentrations of 1.3 and 0.7 ppm Ho, respectively.

In spite of the presence of textures typical of volcanic rocks, and the physical appearance and close association of these felsic and mafic rocks, Easton (1989b) considered the suite to be devoid of volcanic rocks. He introduced the term "pink and black porcelanites" to describe the "andesite" and "rhyolitic tuff" of Hewitt (1968), and claimed that the difference between these is one of color only, not of bulk composition (no bulk-composition data were provided to substantiate this claim). Easton (1989b) did not find definitive volcanic textures in the suite. In his opinion, "the black and pink porcelanites could represent a variety of lithologies, possibly altered and silicified fine-grained sediments, or hydrothermally altered rocks of any number of protoliths that were subsequently silicified". The alteration and silicification were attributed to the emplacement of the Deloro granite. There is no doubt that the original textures described in Appendix 1 are modified and partly obliterated, firstly because of the metasomatic overprint to be documented in this paper, and later, as a result of low-grade metamorphism of the suite. The chemical and mineralogical data presented below can be used to test the proposal of Easton (1989b).

ANALYTICAL TECHNIQUES

Concentrations of the major elements (Table 1) and Ba were determined using X-ray-fluorescence spectroscopy (XRF; Philips PW1400, model 691). Fused glass pellets were run against international standards. The operating conditions were as follows: Rh X-ray tube excited at 40 kV, current 70 mA. Loss on ignition (LOI) was determined by heating pulverized material for 50 minutes at 1000°C. The concentrations of Zr, Y, Nb, Sr and Rb (Table 2) were determined on pressed pellets using the same spectrometer at 70 kV and 40 mA. Instrumental neutron-activation analysis (INAA) was used to determine the concentrations of Hf and eight rare-earth elements (La, Ce, Nd, Sm, Eu, Ho, Yb and Lu) using the Slowpoke-2 nuclear reactor at the Ecole Polytechnique, Montreal. Details of the INAA method were provided by Abdel-Rahman & Martin (1987). Chondrite values used in the normalization of the absolute concentrations of the *REE* are those of the Leedy chondrite (Masuda *et al.* 1973) divided by 1.2 (*cf.* Taylor & Gorton 1977).

The mineralogy of the feldspars present in the whole-rock specimens (1–2 mm^3 of aphanitic

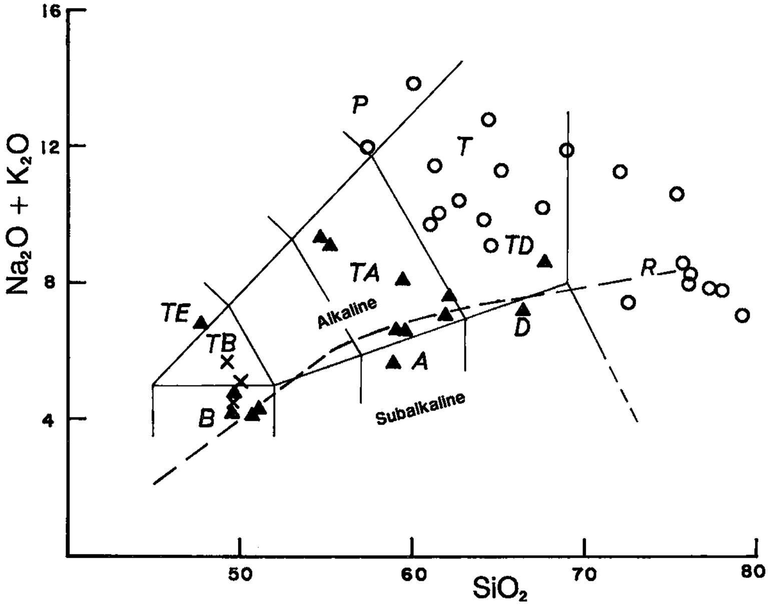

FIG. 2. Composition of the volcanic rocks in terms of ($Na_2O + K_2O$) *versus* SiO_2 (Le Bas *et al.* 1986). Symbols: B basalt, TB trachybasalt, TE tephrite, A andesite, TA trachyandesite, D dacite, TD trachydacite, P phonolite, R rhyolite; crosses: basic volcanic rocks of the Tudor suite; triangles: mafic volcanic rocks, map-unit M; open circles, felsic volcanic rocks, map unit F. Unless otherwise indicated, the symbols in the following figures conform to those in this figure. The dashed line separates fields of alkaline and subalkaline rocks (Miyashiro 1978).

matrix) was determined by X-ray diffraction. A powder pattern recorded using a Guinier–Hägg focusing camera was corrected against a spinel internal standard [a = 8.0833 Å at room temperature, Cu$K\alpha_1$ radiation]. The cell parameters were refined using the program of Appleman & Evans (1973).

GEOCHEMISTRY

Major elements

Whole-rock compositions are presented (Table 1) for 37 samples (15 from unit M and 22 from unit F; sample locations are shown in Fig. 1B). Three samples of the Tudor Formation sampled 12 km northeast of the Deloro complex, north of Queensborough, near the Elzevir batholith, were analyzed for comparison. The 40 bulk compositions are shown in terms of the sum Na_2O + K_2O *versus* silica (Fig. 2). Samples from unit M plot mainly in the fields of basalt, trachyandesite and trachydacite. Only one data point plots in the field of andesite in the IUGS-recommended classification of Le Bas *et al.* (1986), so that the label placed on the unit by Hewitt (1968) is inaccurate.

Samples from the felsic unit (F, Figs. 1A, B) plot predominantly in the fields labeled T (trachyte) - TD (trachydacite) and R (rhyolite); the two samples marginally inside the phonolite field are not silica-undersaturated (quartz is present). Most of the data points plot in the field of alkaline-series volcanic rocks of Miyashiro (1978), *i.e.*, above the dashed line in Figure 2. Some of the data points refer to metasomatized rocks, as hinted at earlier. Because the most important metasomatic reaction involves the exchange of one alkali for the other, with the sum of alkalis remaining constant (see below), a classification based on total alkalis as a function of SiO_2 content gives a reliable indication of the volcanic rock-types present in the Deloro complex.

The felsic suite displays a crudely negative slope in terms of (Na_2O+K_2O) *versus* SiO_2 (Fig. 2). Also, some of the most silicic rocks contain more than 75 wt.% SiO_2. Both features are attributed to the deposition of SiO_2 in pore spaces that developed as a result of devitrification in the originally glassy rocks. The net addition of Si to the most evolved rocks in the suite has led to a decrease in the relative proportion of all other elements, including Na and K. A similar negative slope was documented in a study of rhyolitic tuffs of the Harvey volcanic suite in New Brunswick (Payette & Martin 1986), and ascribed to silicification.

In spite of the metasomatic adjustments in some rocks, the proportion of quartz, albite and orthoclase in the norm (wt.%), and their sum, *i.e.*, the Differentiation Index (DI: Thornton & Tuttle 1960), still provide useful indications of compositional variation in the suite. The DI ranges from 36 to 83 in rocks taken from unit M, and from 76 to 98 in rocks from unit F (Table 1).

The three samples of Tudor metavolcanic rocks are low in SiO_2, as was found by Van de Kamp (1968), and plot in the field of basalt and

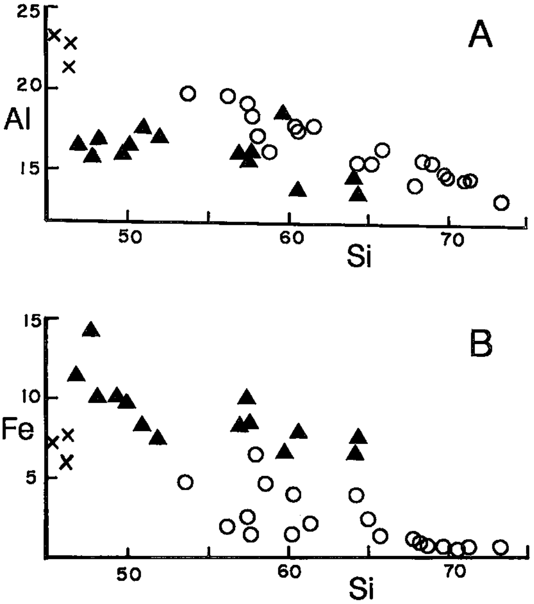

FIG. 3. Composition of the volcanic rocks in terms of Si *versus* Al (A), and of Si *versus* Fe (B). Values in cation %.

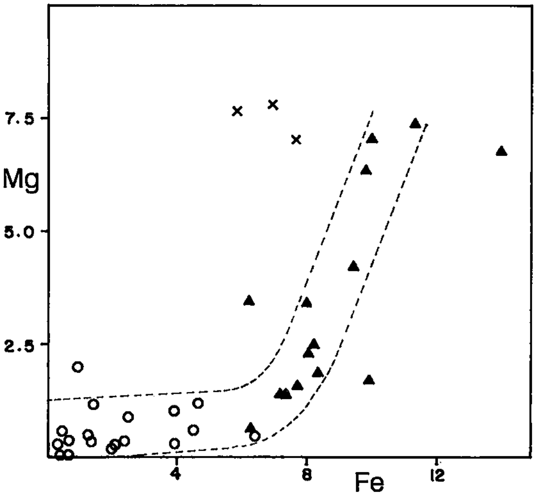

FIG. 4. Composition of the volcanic rocks in terms of Mg *versus* Fe. Values in cation %.

trachybasalt. These rocks are distinguished by a lower Si content than the most basic rocks of unit M. Also, they are distinctly richer in Al and poorer in Fe than the basic rocks of unit M (Figs. 3, 4), as might be expected of volcanic rocks of calc-alkaline affinity (Fig. 5). Plots of Al and Fe *versus* Si (Fig. 3) suggest that the volcanic rocks in the Deloro suite belong to one of two groups: basalt – trachydacite (lower Al, higher Fe), and trachyte – rhyolite (higher Al, lower Fe).

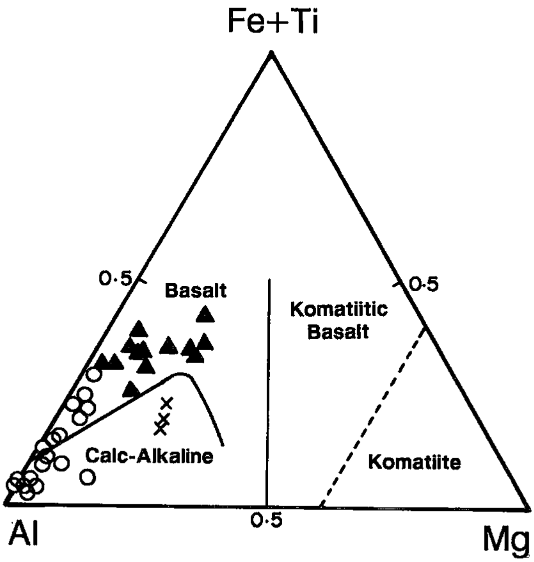

FIG. 5. Composition of the volcanic rocks in terms of the Mg – (Fe + Ti) – Al discriminant diagram (after Jensen 1976). Plot displays molar proportions.

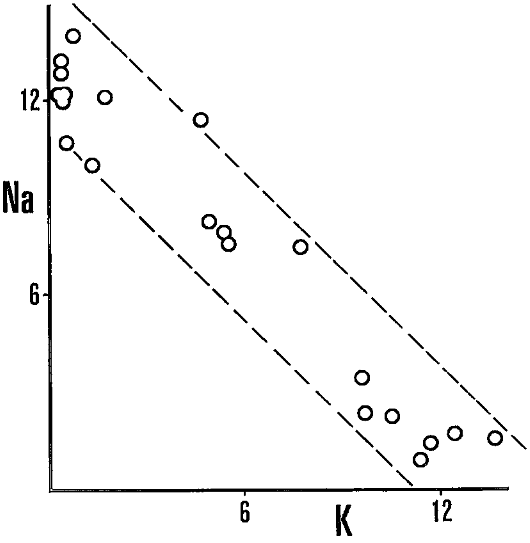

FIG. 6. Composition of the felsic volcanic rocks in terms of Na and K (molar basis).

Rocks of the felsic unit contain much less Mg and Fe than those of unit M (Fig. 4). The felsic rocks probably are interrelated by a process of crystal fractionation (see below). The most Mg-rich rocks of unit M are not sufficiently rich in Mg to be considered primitive. The more evolved rocks of unit M may result by mixing with the felsic magma. Together, the felsic and mafic units define a typical basalt – rhyolite suite in terms of Mg – (Fe + Ti) – Al (Fig. 5). In contrast, the three samples of the Tudor Formation plot in the field of calc-alkaline rocks in Figure 5. These three samples seem similar to the much larger suite studied by Sethuraman & Moore (1973) and Condie & Moore (1977), who concluded that the Tudor volcanic suite in the Bishop Corners – Donaldson area, located 50 km northeast of Madoc, consists of mafic to intermediate members of a dominantly calc-alkaline association in which low-K tholeiitic basalts also are found.

Many of the samples of the trachyte – rhyolite unit show evidence of the former presence of glass. Petrographic evidence for its devitrification (*e.g.*, the development of a spherulitic texture) is clear. The process is known to be triggered by the introduction of hot water along contraction cracks (*e.g.*, Lofgren 1971). Sodium, potassium, ^{18}O and Ar are particularly prone to mobilization as the glass is altered (*e.g.*, Cerling *et al.* 1985) and transformed to an intergrowth of quartz and the two feldspars, one K-rich, the other Na-rich. The erratic proportions of K and Na in the rhyolitic and trachytic rocks of unit F (Table 1) are considered the result of such local remobilization; it has given rise to extremes in composition within a short distance in unit F. For example, samples F15, F18 and F20 are ultrapotassic, whereas samples F5, F14 and F16 are ultrasodic. These chemical features are considered to result from a circulating fluid phase following emplacement. The total of the alkalis did not change significantly as a result of the ion-exchange reaction (Fig. 6). The data points in Figure 6 conform to an envelope of slope −1, the trachytic samples containing a greater proportion of Na + K than those of rhyolitic composition. Such an exchange reaction is likely to have been rapid, as it does not involve a concomitant change in the Al–Si framework.

The ratio (Na + K)/Al, or the agpaitic index, is a measure of alkalinity of a felsic rock. As devitrification proceeded in a hydrothermal environment, the index may well have decreased slightly as a result of the preferential removal of the alkalis. All felsic volcanic rocks have an index less than 1, but some are so close to 1 (F6, F7, F9; Table 1), like the granophyric granite at Deloro, that they probably

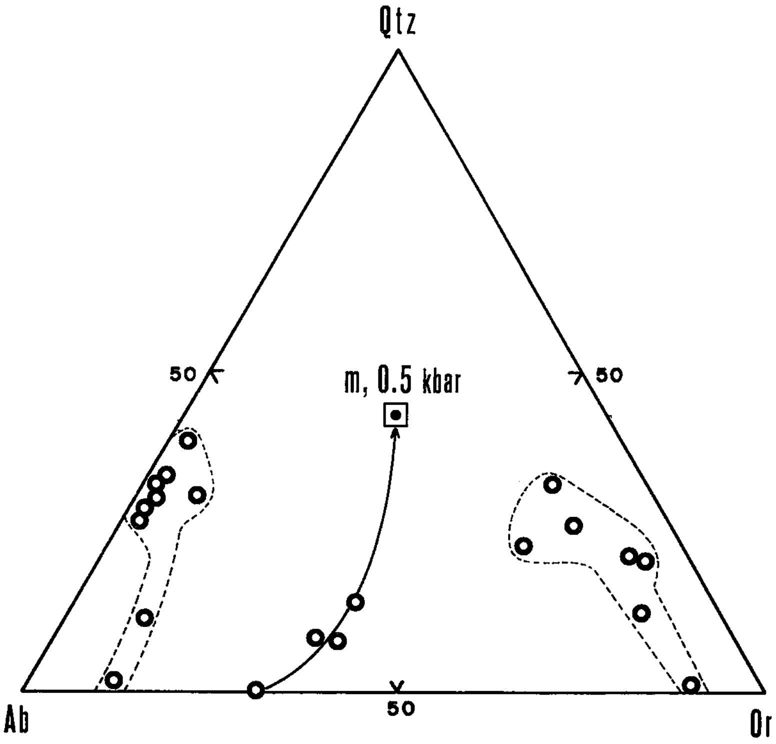

FIG. 7. Composition of the felsic volcanic rocks (DI > 80) in terms of normative quartz, albite and orthoclase (wt. %). Also shown are the 0.5 kbar minimum in the water-saturated haplogranite system and the experimentally determined path to be followed by a trachytic liquid fractionating a single alkali feldspar and evolving toward the quaternary minimum (both taken from Tuttle & Bowen 1958).

did exceed 1 prior to exposure to a fluid phase. Note that the index is not affected by the exchange of Na and K that occurred in some rocks. Volcanic analogues to the medium-grained peralkaline granite have not been encountered.

The great variability among the felsic rocks can best be illustrated in a triangular diagram showing the normative constituents Qtz, Ab and Or for those rocks in which the DI exceeds 80 (Fig. 7). Four samples that are relatively poor in normative quartz contain normative albite and orthoclase roughly in the proportion 60:40, and plot close to a possible path of fractionation determined at a $P(H_2O)$ ($= P_{total}$) $= 0.5$ kbar by Tuttle & Bowen (1958); this pressure is judged to have been appropriate for the emplacement of the volcanic rocks. We contend that these four bulk compositions are close to the composition of the magma frozen upon eruption.

Of the twenty bulk compositions plotted in Figure 7, nine are strongly Na-enriched and depleted in K, whereas seven are strongly K-enriched and depleted in Na. This dichotomy was not realized at the time of the field work; the exchange did not lead to any obvious changes in the appearance of the hand specimens.

None of the samples that are enriched in SiO_2 content lies on the fractionation trend shown in Figure 7. This absence is not likely due to pure chance during sampling. We contend that the porosity and permeability of the predominantly rhyolitic products of devitrification were much greater than those of the trachytic samples, which predominantly show a flow-induced trachytic texture and which contained a much lower proportion of glass. The porosity of the microcrystalline assemblages is attributed mainly to differential rates of thermal contraction of quartz and the two feldspars present at the outset of the devitrification process.

Trace elements

The concentrations of trace elements in the volcanic rocks should be considered as the cumulative result of magmatic processes and the metasomatic overprint. The concentration of high-field-strength elements such as Zr, Nb and Y (Table 2) in the felsic rocks (DI > 80) does not show a dependence on K/(K + Na). Data points scatter about the median values 250 ppm Zr, 20 ppm Nb, and 50 ppm Y (these plots are not shown). For comparison, the granophyric granite in the plutonic part of the complex contains 310 ppm Zr and 102 ppm Y (average

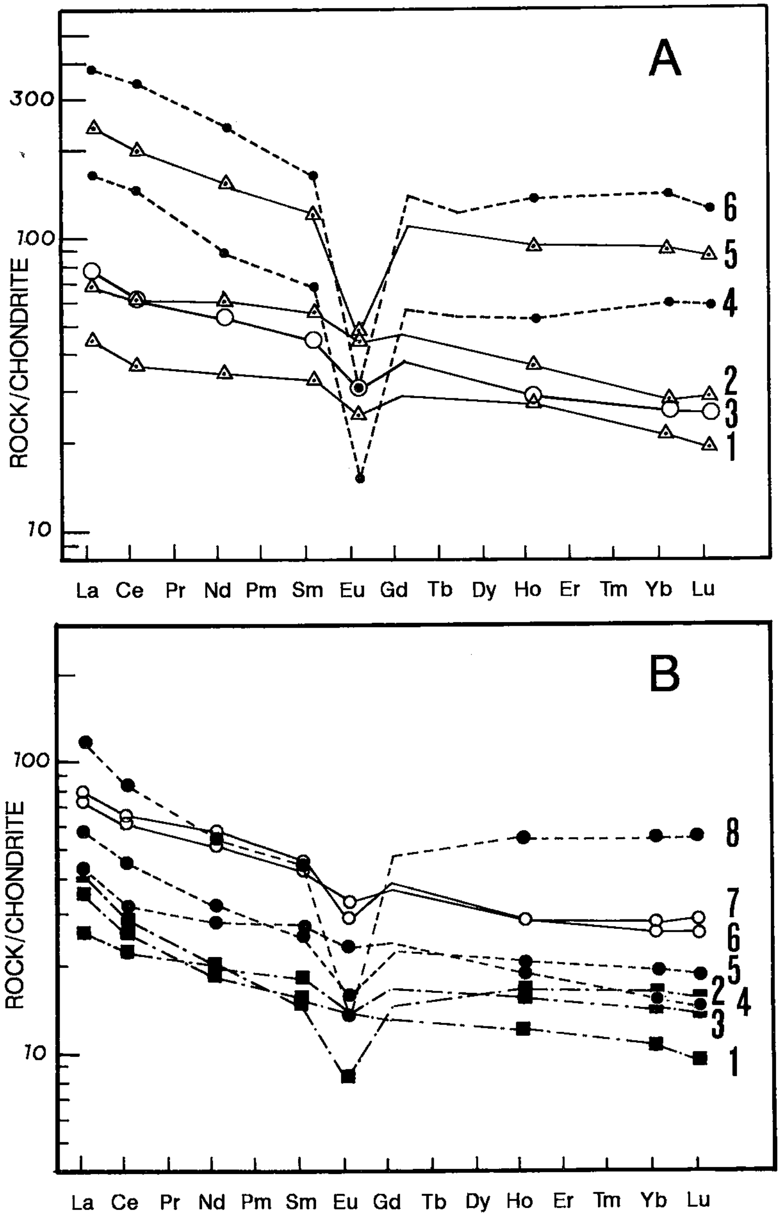

FIG. 8. A. Chondrite-normalized rare-earth profile of rocks from unit M. Profiles: 1 basalt M6 (DI = 45), 2 trachyandesite M13 (DI = 64), 5 "dacite" M18 (DI = 76). Profiles 3, 4 and 6 are shown for comparison; 3 represents an average of two compositionally undisturbed quartz trachytes (F3, F11; DI = 80), 4 is an average profile of the granophyric granite (DI = 95), and 6 is that of the peralkaline granite (DI = 93). Profiles 4 and 6 are taken from Abdel-Rahman & Martin (1987). B. Rare-earth profile of rocks from unit F: 1 F16 [DI = 85, K/(K+Na) 0.12], 2 F8 (83, 0.29), 3 F12 (90, 0.88), 4 F5 (98, 0.03), 5 F20 (87, 0.90), 6 F11 (78, 0.37), 7 F3 (82, 0.42), 8 F15 (98, 0.80).

of two samples; Table 1 in Abdel-Rahman & Martin 1987).

In contrast to these elements, the concentration of low-field-strength elements, such as Rb and Ba, likely is "reset" during the ion-exchange reaction. The Rb content of the felsic rocks increases from less than 10 ppm where K/(K + Na) is less than 0.05 to 200 ppm where K/(K + Na) is 0.9. Similarly, the concentration of Ba is <10 ppm where K/(K + Na) is <0.05, and increases to a value in the range 800–1400 ppm where K/(K + Na) is 0.9. Some scatter is to be expected in such plots, as the felsic starting material for the ion-exchange reaction is not fixed, but varies in the proportion of quartz to feldspar (which is the carrier of Rb and Ba). The original concentration of Rb and Ba presumably lies near the middle of these ranges, and close to values typical of the granophyric granite, with which the felsic volcanic products are considered genetically linked on textural, mineralogical and geochemical grounds. The granophyric granite, which does approach its primary K/(K + Na) value more closely than most felsic volcanic samples, contains 90 ppm Rb and 380 ppm Ba, levels of concentration that lie almost exactly in the middle of the respective ranges.

During the metasomatic adjustments in these felsic volcanic rocks, it is clear that Rb and Sr became uncoupled. There is a subtle buildup in Sr concentration, from 100 to 160 ppm, as K in the feldspar is progressively replaced by Na, but in the most extreme cases of albitization, Sr concentrations drop to 65 ± 20 ppm. This uncoupling of Rb and Sr probably is not responsible for the important disturbances that have been documented in the Rb–Sr isochron (reviewed by Abdel-Rahman & Martin 1987) because 1) the open-system behavior affected the cooling volcanic pile only, as revealed by a complementarity in the alkali-exchanged products, and 2) the metasomatic exchange occurred largely as a result of devitrification, and thus as the complex cooled. The important disturbances in the Rb–Sr system occurred 150 and 800 Ma after the metasomatic exchanges documented above, but most likely were abetted through the development of secondary porosity at the deuteric stage.

Hewitt (1968) described a sample of the basic volcanic member of the association as "very fresh andesite composed of elongate laths of hornblende and finely intergrown andesine feldspar". His representative sample contains 48.96% SiO_2, 3.37% Na_2O and 1.00% K_2O. In view of our petrographic observations (Appendix 1) and information on the chemical composition (Table 1) and the feldspar mineralogy of two representative samples from this unit (see below), it seems likely that such "very fresh" samples contain a fresh-looking subsolidus assemblage. Sample M6 contains 47.74% SiO_2, 1.56% Na_2O, and 5.16% K_2O, whereas M13 contains 55.20% SiO_2, 8.06% Na_2O and 1.04% K_2O. Such levels of alkalis probably result from interaction of hot basic rocks with the alkali-bearing fluids involved in the metasomatism of the felsic rocks. The following broad ranges of concentration (in ppm) characterize rocks having a differentiation index less than 80 (Table 2): Rb 7–256, Ba<10–1171, Sr 4–310, Zr 163–1309, Nb 16–38, Y 22–194, Hf 5–36.

The rare earths

For convenience, the chondrite-normalized rare-earth-element plots are presented separately for the more mafic rocks, *i.e.*, unit M (DI 45, 64, 76; spectra 1, 2 and 5 in Fig. 8A), and for eight samples representative of the felsic rocks in unit F (DI in the range 78–98; Fig. 8B). Figure 8A also includes an average profile of two relatively undisturbed rhyolites (pattern 3; average of 6 and 7 in Fig. 8B), an average profile of the granophyric granite (pattern 4, $n = 2$) and peralkaline hypersolvus granite (pattern 6, $n = 5$). Profiles 4 and 6 are reproduced from Abdel-Rahman & Martin (1987, Table 2; sample P8–139 contains 1.7 ppm Lu, not 0.17 ppm as stated there).

Patterns for basalt M6 and trachyandesite M13 (1,2, Fig. 8A) are subparallel and of similar overall aspect. Both exhibit a relatively flat, unfractionated pattern among the light rare-earths (La/Sm_n 1.2, 1.3), and a small negative Eu anomaly. In both respects, these less evolved rocks closely resemble the syenites exposed in the western part of the complex (Abdel-Rahman & Martin 1987). The sequence basalt – trachyandesite – syenite shows an increase in total concentration of the rare earths [Σ8*REE* 80 (M6), 133 (M13), 249 ppm (average of 6 syenites)]. Such a buildup is expected to result from crystal fractionation; the influences of magma mixing and metasomatism are at present unknown.

Spectra 4, 5 and 6 (Fig. 8A) show an increasing enrichment in the rare earths, especially in the light rare-earths (La/Sm_n 1.94 in "dacite" M18, 2.26 in peralkaline granite, 2.41 in granophyric granite); the spectra also show a pronounced negative Eu anomaly, which presumably results from the progressive fractionation of feldspar in the sequence "dacite" (5), peralkaline granite (6), granophyric leucogranite (4). The sequence of increasing differentiation index is 5 – 6 – 4 (with values of 76, 93, 95), not 4 – 5 – 6, as might have been predicted from increasing rare-earth concentrations. The depletion in rare earths in the granophyre is likely a reflection of the efficient fractionation of a *RE*-bearing accessory phase near the final stage of crystallization of the leucogranitic magma.

Part of the felsic magma had a trachytic composition, and thus seems genetically linked to the syenitic plutonic facies. The rare-earth profile of the trachytes is rather primitive, using as criteria the shallowness of the negative Eu anomaly and the low concentrations of the rare earths. Samples F3 and F11, represented by pattern 3 (Fig. 8A), have an undisturbed (in terms of Na and K; see below) trachytic composition. Their pattern is intermediate between those of basalt and trachyandesite.

The separate patterns for F3 and F11, shown in Figure 8B (7 and 6, respectively), constitute a useful reference point for the comments that follow because they are 1) trachytic and 2) undisturbed in their Na/K value. Sample F15 (8, Fig. 8B) represents a high-silica, K-metasomatized rhyolite. It has the same concentrations of the heavy rare-earths, equivalent negative europium anomaly, and the same $\mathrm{La/Sm_n}$ value as the granophyric leucogranite (4, Fig. 8A), but is systematically depleted in the light rare-earths. There are two possible explanations for the depletion: 1) fractionation of a *LREE*-bearing accessory in the transition from the leucogranitic magma that produced the granophyric granite (DI 95) to that responsible for F15 (DI 98), or 2) selective removal of the light rare-earths during the exchange of K for Na.

The ambiguity can be evaluated by examining the pattern of two more intensely K-metasomatized rhyolites (F12, F20; 3 and 5 in Fig. 8B). On the basis of their DI (which is not significantly affected by K-for-Na exchange), an assumption can be made that these rhyolites had a profile intermediate between patterns 5 and 6 in Figure 8A. The low concentration of the rare earths, which makes these rhyolites resemble basalt M6 (1, Fig. 8A), and the anomalous cross-over in the curves in the region of the light rare-earths, suggest that intense K-for-Na exchange in the feldspar is accompanied by generalized loss of most rare earths. However, this statement cannot be made stronger, because of an inherent ambiguity in the metasomatic evolution of the samples (see Discussion).

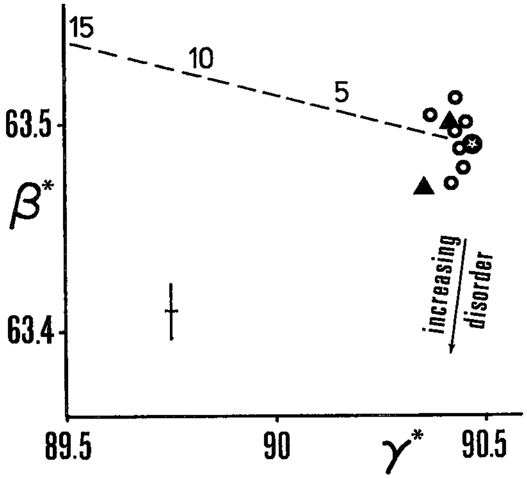

FIG. 9. A portion of the β^* - γ^* plot (Smith 1974) showing the position of the sodic plagioclase from samples M6, M13, F3, F5, F8, F11, F14, F15 and F16 with respect to end-member ordered albite (encircled star). The dashed line marks the locus of ordered structures in the range $\mathrm{An_0}$ to $\mathrm{An_{15}}$. A decrease in the degree of Al–Si order causes a decrease in the value of β^*. Also shown is an average standard error for the samples plotted. The standard errors are provided by the program of Appleman & Evans (1973).

Rhyolite F16 (1, Fig. 8B) contains an anomalously low concentration of all rare earths, lower even than the basalt (1, Fig. 8A). In addition, there is no Eu anomaly, as there is in all the other samples. This rhyolite has been subjected to Na-metasomatism; we postulate that most rare earths were partly removed as the K-feldspar was transformed into albite, presumably owing to the destabilization of an accessory phase.

Data for two more Na-metasomatized felsic rocks (F5, F8; 4 and 2 in Fig. 8B) are presented for comparison with F16. Sample F5 is the most strongly Na-metasomatized of all three. As a group, these three rocks are the most strongly depleted in the rare earths of the entire suite. As all three rocks did not share the same precursor, a correlation cannot be established between enrichment in Na and depletion in the rare earths. There seems to be no doubt, however, that the rare earths are not as inert as some high-field-strength elements, such as Zr and Nb, discussed earlier.

FELDSPAR MINERALOGY OF THE VOLCANIC SUITE

The cell dimensions of the feldspar(s) in two mafic samples (M6, M13) and ten felsic samples (F3, F5, F8, F11, F12, F14, F15, F16, F20 and a gold-mineralized porphyry from an apophysis in the northern part of the complex) are listed in Table 3, which is available at nominal cost from The Depository of Unpublished Data, CISTI, National Research Council of Canada, Ottawa, Ontario K1A 0S2.

The mafic rocks

In terms of volume, the most prominent plagioclase composition in samples M6 (basalt) and M13 (trachyandesite) is albite, $\mathrm{An_1}$. This inference is based on location in the β^* - γ^* plot (Fig. 9). The small amount of residual disorder in the albite from the basalt is typical of that in albite formed by the albitization of plagioclase (Martin 1984). There is no evidence for a more calcic plagioclase or a K-rich feldspar in the X-ray-diffraction pattern. The coexistence of albite, calcite, and other Ca-bearing phases

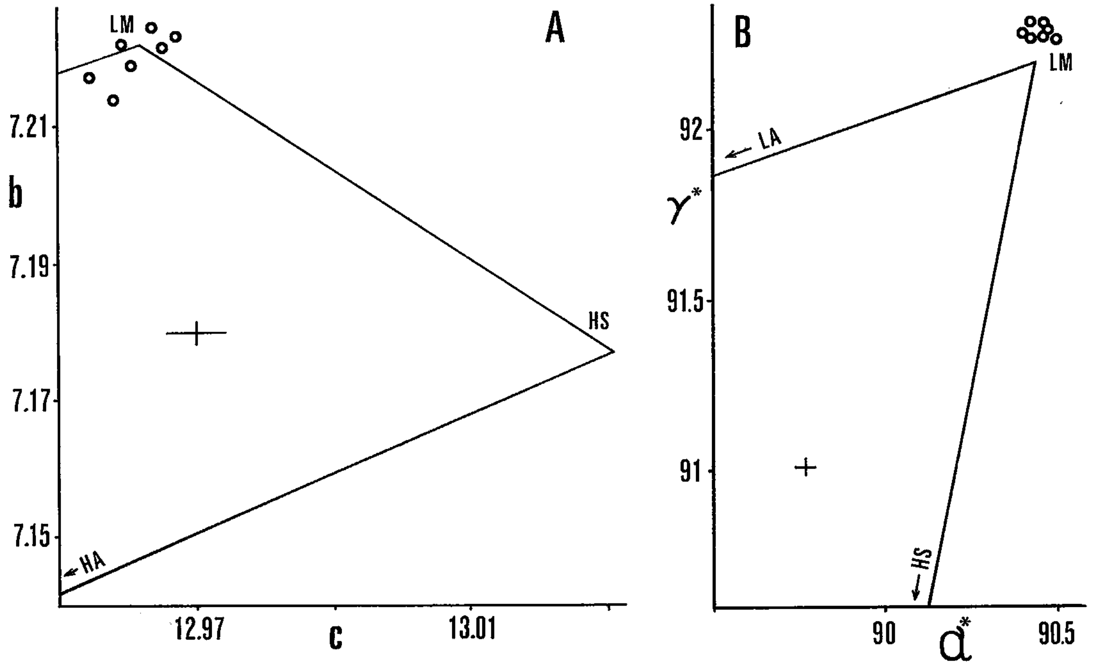

FIG. 10. A. A portion of the b - c quadrilateral showing the distribution of the microcline data-points. LM low microcline, HS high sanidine, HA high albite. B. A portion of the α^* - γ^* plot showing the location of the microcline data-points with respect to the LM corner. LA low albite. Raw data are reported in Table 3.

is consistent with re-equilibration below 400°C, according to the phase diagram for the system Ab–An (Smith & Brown 1988, Fig. 1.4), and thus in the greenschist facies. In both rocks, the high concentration of Na and K suggests that albitization of the primary plagioclase occurred during the course of alkali metasomatism.

The felsic rocks

The great variability in the bulk composition of the trachytic and rhyolitic rocks (Fig. 7) is a consequence of variability in the proportion of K-rich and Na-rich feldspars. The least disturbed rocks contain the assemblage low microcline - low albite; the disturbed rocks contain low microcline without low albite or low albite without low microcline.

As in much of the plutonic suite (Abdel-Rahman & Martin 1987), the microcline is very well ordered (Figs. 10A, B) and has a composition in the range Or$_{97-99}$; in all cases but one, t_1O, the proportion of Al in the T_1O position, is 0.99 or 1 (Table 4). A less well ordered and more sodic microcline is present in the Au-mineralized quartz porphyry. The microcline is invariably slightly anomalous in its value of γ^*, which exceeds that of end-member low microcline by more than one standard deviation (Fig. 10B).

TABLE 4. INDICATORS OF COMPOSITION AND DEGREE OF Al-Si ORDER, K-RICH FELDSPAR IN MATRIX OF TRACHYTE AND RHYOLITE

		$\underline{N}_{Or}$	$\underline{t}_1$O+$\underline{t}_1$m	$\underline{t}_1$O−$\underline{t}_1$m	$\underline{t}_1$O	Δ
F3 trachyte	LM	97.1	0.981	0.989	0.99	0.97
F8 trachyte	LM	97.5	0.984	0.987	0.99	1.00
F11 trachyte	LM	99.0	1.009	1.010	1.01	0.99
F12 trachyte[1]	LM	97.6	1.009	0.984	1.00	0.99
F15 rhyolite	LM	97.9	0.987	1.001	0.99	1.01
F20 trachyte	LM	99.0	0.994	1.003	1.00	0.97
Au porphyry[1]	LM	95.7	0.953	0.972	0.96	1.00

Composition $\underline{N}_{Or}$ is expressed in mole % Or, and was calculated using the equations of Kroll & Ribbe (1983) for the ordered (LM-LA) series. Degree of Al-Si order, expressed by $\underline{t}_1$O, was computed using the equations of Blasi (1977). The error in $\underline{N}_{Or}$ and $\underline{t}_1$O is believed to be ±0.015 in most cases. Symbols: LM low microcline, LA low albite; the obliquity Δ is equal to 12.5($\underline{d}_{131}$ - $\underline{d}_{1\bar{3}1}$). Au porphyry: a gold-mineralized hydrothermally altered quartz porphyry (not analyzed chemically). The names listed for the other samples reflect their position in the (Na_2O + K_2O) versus SiO_2 plot (Fig. 2), except that F20 is called a trachyte instead of a phonolite. All samples contain quartz. [1] The sample is devoid of albite. Muscovite is present with the microcline in the Au-mineralized porphyry. In sample F20, the assemblage is microcline + albite is present, but the proportion of albite is very small (there is insufficient material for a cell refinement, and thus no entry for F20 in Table 5).

The data show that the felsic rocks have reached compositional and structural equilibrium at a low subsolidus temperature, even below 200°C (*cf.* the K-limb of the strain-free alkali feldspar solvus; *cf.* Smith & Brown 1988, Fig. 1.2; Brown & Parsons 1989, Fig. 8a). These rocks have equilibrated more completely than the plutonic rocks, in which less well ordered microcline may be found. The microcline

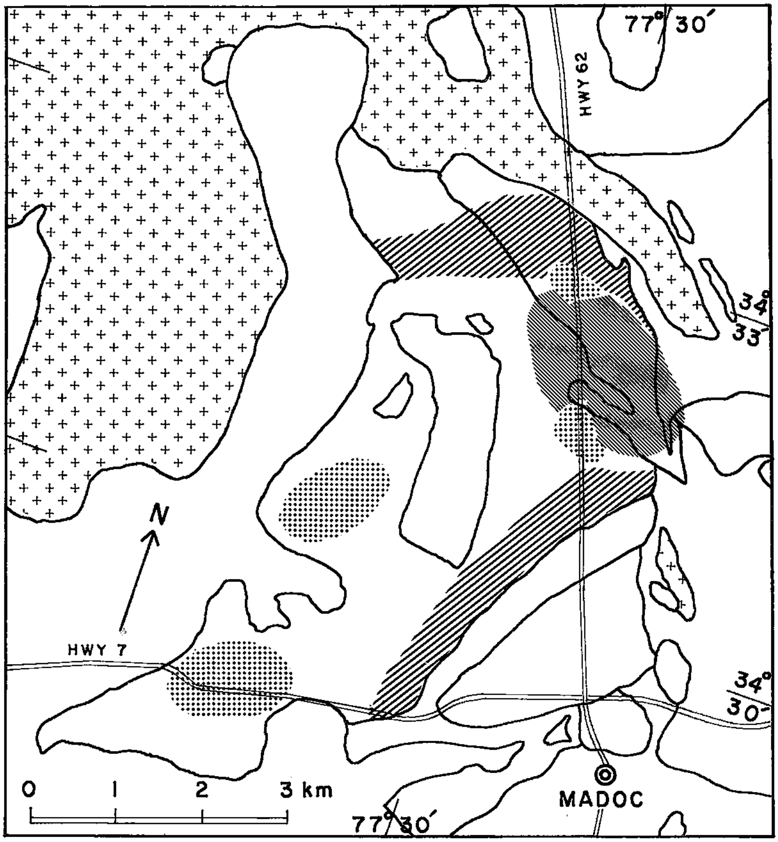

FIG. 11. Map showing the distribution of relatively unmetasomatized (dot pattern), Na-metasomatized (thick-line hachures), and K-metasomatized volcanic rocks (thin-line hachures). Rock units and geological boundaries are the same as in Figure 1B.

TABLE 5. COMPOSITION AND ESTIMATE OF DEGREE OF Al-Si ORDER, Na-RICH FELDSPAR IN MATRIX OF MAFIC AND FELSIC VOLCANIC ROCKS

	An	$\underline{t}_1o+\underline{t}_1m$	$\underline{t}_1o-\underline{t}_1m$	$\underline{t}_1o$	Δ131
M6 basalt	1	0.955	0.955	0.96	1.135
M13 trachyand.	0	0.989	0.982	0.99	1.113
F3 trachyte	0	0.993	0.997	1.00	1.101
F5 rhyolite[1]	0	0.982	0.995	0.99	1.106
F8 trachyte	1	0.971	0.962	0.97	1.133
F11 trachyte	0	1.013	0.986	1.00	1.111
F14 trachyte[1]	0	0.986	0.984	0.99	1.103
F15 rhyolite	0	0.993	1.004	1.00	1.121
F16 trachyte[1]	0	0.994	0.983	0.99	1.107

The An content was estimated from the $\beta^* - \gamma^*$ plot of Smith (1974, Fig. 7-44). In all cases, the albite is very close to the curve that describes ordered structures in this diagram. The apparent degree of order is expressed by $\underline{t}_1o$, which also is affected by small amounts of the An component in the plagioclase (e.g., in M6 and F8). The calculated angular separation of the 131 and $1\bar{3}1$ reflections ($CuK\alpha_1$ radiation), Δ131, is expressed in degrees. Among felsic rocks, microcline is absent in samples denoted by [1]; in trachyte F16, the albite coexists with muscovite, and its cell parameters are given in Table 3. The names assigned to samples reflect their position in a plot of (Na_2O + K_2O) *versus* SiO_2 plot (Fig. 2), except that M6 is called basalt instead of tephrite. Quartz is present in all samples.

in "microclinites" F12 and F20 is indistinguishable from that in the two-feldspar assemblages. The slight departure from perfect Al–Si order and the higher Na content of the microcline in the Au-mineralized porphyry are consistent with a higher temperature of final equilibration (closer to 300°C?).

The albite in the felsic rocks has a composition in the range An_{0-1}, and plots within one standard deviation of the curve describing ordered structures (Fig. 9). The albite in rocks devoid of microcline ("albitites" F5, F14, F16) is indistinguishable from that in the two-feldspar rocks.

DISCUSSION

Hewitt (1968) assigned the so-called "Madoc volcanics" to the regionally distributed Tudor suite of metabasalt and meta-andesite. Exposures of the Tudor volcanic rocks occur within 3 km to the east of the Deloro complex. The felsic and mafic volcanic rocks that are spatially associated with the Deloro complex are distinct from the Tudor suite and, as described above, are considered to form part of the anorogenic complex (Fig. 1A). Like Easton (1989a), we favor the abandonment of the term "Madoc volcanics" (but obviously not for the same reason). As in other examples of such complexes, the volcanic suite presumably has been preserved because of foundering of the roof upon evacuation of the magma reservoir (Smith & Bailey 1968).

The volcanic members of the Deloro complex bear a close relationship to the geochemically and mineralogically distinctive plutonic members. The felsic volcanic products emplaced directly above the intrusive body, roughly 1240 Ma ago, underwent major metasomatic changes during cooling. The local thoroughness of these changes is consistent with the upwelling of a relatively high-temperature hydrothermal phase issued from the cooling epizonal plutonic complex, located immediately under the volcanic cover. In the light of experiments involving a thermal gradient, an exchange of Na for K can be expected in the high-temperature regime (*e.g.*, Orville 1963). The complementary K-for-Na exchange reaction can be expected to occur in the lower temperature region of a circulating system.

The distribution of Na- and K-metasomatized volcanic rocks is shown in Figure 11. Although large areas are left blank owing to lack of outcrop, a pattern does emerge: an area of K-metasomatized rocks is flanked by two areas of Na-metasomatized rocks. The pattern of distribution could well result from a two-stage development of metasomatic interaction of volcanic rock and fluid. At first, generalized Na-metasomatism is believed to have occurred along an arcuate zone of hydrothermal activity along which Na was removed from the fluid and K was removed from the rocks. At a lower temperature, in the waning stage of hydrothermal circulation, the reverse ion-exchange reaction, *i.e.*, removal of K from the fluid and of Na from the rocks, seems to have become constricted to a single zone. In our reconstruction, an overprint of lower-temperature K-metasomatism thus was superimposed on the earlier sodic products. This pattern has been documented in other examples of epizonal anorogenic felsic magmatism (*e.g.*, Bowden *et al.* 1987).

The feldspar mineralogy of the volcanic suite indicates the attainment of the thermodynamically stable assemblage low microcline + low albite. The degree of Al–Si order of the microcline indicates efficient recrystallization below 400°C (*e.g.*, Brown & Parsons 1989, Fig. 8a), whereas compositions of coexisting low microcline and low albite recorded in Tables 4 and 5, respectively, are consistent with equilibration below 200°C. We did not encounter slight departures from the equilibrium degree of Al–Si order, as were found to persist in the plutonic suite. The more uniform approach to equilibrium in the volcanic rocks is considered to result from 1) the fine grain-size and 2) the greater permeability of these rocks, as a result of devitrification and recrystalli-

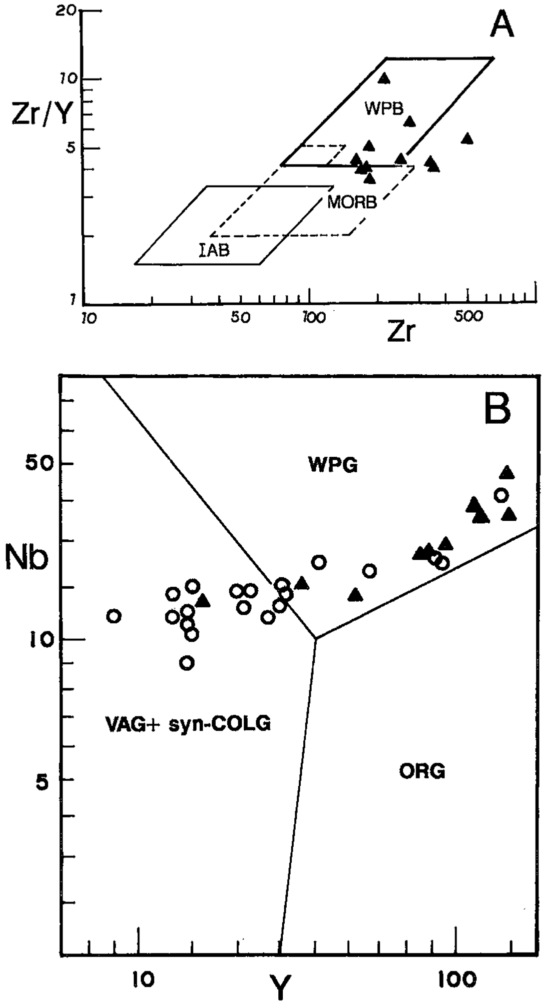

FIG. 12. A. Composition of the more basic rocks of unit M, plotted in terms of Zr/Y *versus* Zr concentration (in ppm). The 11 samples plotted are basalts or trachyandesites; samples containing more than 60 wt.% SiO_2 are not shown on this diagram. The fields of within-plate basalts (WPB), mid-ocean ridge basalts (MORB), and island-arc basalts (IAB) are taken from Pearce & Norry (1979). B. Composition of the felsic and intermediate volcanic rocks in terms of Nb *versus* Y concentrations (in ppm). Samples of basaltic composition (47–55 wt.% SiO_2) are excluded. The fields of within-plate granite (WPG), volcanic-arc granite (VAG) and syncollisional granite (syn-COLG), and ocean-ridge granite (ORG) are those of Pearce *et al.* (1984). The data points in the VAG + syn-COLG field pertain to metasomatized samples; both Na-metasomatized and K-metasomatized samples seem similarly depleted in Y.

zation. As in the case of the plutonic rocks, however, the main reason for the occurrence of low microcline in these volcanic rocks (as opposed to less well ordered microcline) probably lies in the fact that the entire complex has been mildly reheated twice, firstly 150 Ma, then 800 Ma after emplacement and initial cooling. Abdel-Rahman & Martin (1987) reviewed the evidence for these regional events. The thoroughness of the metasomatic changes in the affected rocks argues strongly in favor of their occurrence when the rocks first cooled, 1240 Ma ago, rather than as a result of the younger events.

The oxygen-isotope data of Wu & Kerrich (1986) are entirely consistent with our interpretation of thorough low-temperature hydrothermal re-equilibration in the volcanic assemblage. In the rhyolitic rocks, they found $\delta^{18}O$ values in the range 11.7 to 14.2‰, whereas samples of the peralkaline hypersolvus granite lie in the range 9.1 to 11.8‰ , and gabbro from the western part of the Deloro complex, barely affected by the hydrothermal overprint, gives a typical magmatic $\delta^{18}O$ value of 7.1‰ . A complicated petrogenetic scheme advocating different source-areas could be proposed to explain these data (hypothesis 2 of Wu & Kerrich 1986). The simpler hypothesis, that all rocks once had a magmatic $\delta^{18}O$ value, but that the felsic plutonic rocks in the core of the pluton, and especially their extrusive equivalents on the eastern side, underwent a very important hydrothermal chapter in their petrogenetic history, is well supported by the mineralogical and chemical changes documented herein.

In view of the importance of widespread open-system behavior in the volcanic products of this complex, little can be said concerning processes at the magmatic stage. Felsic and mafic magmas both erupted, and may have mixed locally. The exact relationship between primitive (mafic) melts, which were responsible for the gabbroic portion of the complex and for the coeval Cordova complex 10 km to the west, and the more felsic magma of trachytic to rhyolitic composition, cannot be answered without further investigations, which must focus on unmetasomatized samples. The presence of a negative Eu anomaly indicates that plagioclase and, in the more evolved melts, Ca-bearing sanidine formed part of the fractionating assemblage, as in the case of the plutonic suite. Also, the fractionation of a calcic amphibole may have led to the efficient enrichment in silica and the alkalis (Bonin & Giret 1984), leading ultimately to the development of leucogranitic melts. An evaluation of the relative importance of mixing with a melt formed by the anatexis of supracrustal rocks, considered to be a likely adjunct to crystal fractionation in the plutonic suite by Abdel-Rahman & Martin (1987), cannot be addressed with the data acquired on the volcanic products.

The anorogenic tectonic setting of the volcanic products, inferred from data on the plutonic rocks, can be checked using discriminants based on trace-element concentrations. In view of the importance of alkali metasomatism in part of the Deloro volcanic suite, however, only the least mobile elements can be expected to provide useful indications. In terms of Zr/Y *versus* Zr (Fig. 12A), basalts and the less siliceous trachyandesites plot in the area of within-plate basalts (WPB), as defined by Pearce & Norry (1979), but half the points are outside the WPB field, principally in the direction of increasing Zr concentration. In a plot of Nb *versus* Y (Fig. 12B), trachydacitic and trachyandesitic samples from the area mapped as the mafic unit plot in the field of within-plate felsic and intermediate rocks, as defined by Pearce *et al.* (1984). Whereas some samples of trachytic or rhyolitic composition also plot in the field of within-plate granites, most spill over into the area of volcanic-arc and syncollisional granites. Most of the aberrant points refer to alkali-exchanged bulk compositions. We conclude, therefore, that although Nb is relatively immobile, the concentration of Y (as well as the *REE*) in these rocks was reduced as a result of alkali metasomatism. Earlier, we pointed out that concentrations of Y show no dependence on K/(K + Na) value in the felsic rocks. Such differential subsolidus mobility of the high-field-strength elements and the rare earths must result from differing stability relationships among the accessory phases that host these elements.

ACKNOWLEDGEMENTS

We thank Professor John Ludden (Université de Montréal) and Mr. Gilles Gauthier (Ecole Polytechnique, Montréal) for assistance with the neutron-activation analyses. Mr. S.T. Ahmedali facilitated the acquisition of major- and minor-element data using the X-ray-fluorescence technique. Research costs were covered by a grant (A7721) from the Natural Sciences and Engineering Research Council to RFM. We thank Dr. J.M. Moore Jr., an anonymous referee and Acting Editor J.L. Jambor for useful remarks and a critical reading of an earlier version of this paper.

REFERENCES

ABDEL-RAHMAN, A.M. & MARTIN, R.F. (1987): The Deloro anorogenic igneous complex, Madoc, Ontario. I. Geochemistry and feldspar mineralogy of the felsic plutonic rocks. *Can. Mineral.* **25**, 321-336.

APPLEMAN, D.E. & EVANS, H.T., JR. (1973): Job 9214: indexing and least-squares refinement of powder diffraction data. *U.S. Geol. Surv. Comput. Contrib.* **20** (NTIS Doc. **PB2-16188**).

Bartlett, J.R., Brock, B.S., Moore, J.M., Jr. & Thivierge, R.H. (1984): Grenville traverse A: cross-sections of parts of the Central Metasedimentary Belt. *Geol. Assoc. Can. Field Trip Guidebook* **9A/10A.**

Blasi, A. (1977): Calculation of T-site occupancies in alkali feldspar from refined lattice constants. *Mineral. Mag.* **41,** 525-526.

Bonin, B. & Giret, A. (1984): The plutonic alkaline series: the problem of their origin and differentiation, the role of their mineralogical assemblages. *Phys. Earth Planet. Int.* **35,** 212-221.

Bowden, P., Black, R., Martin, R.F., Ike, E.C., Kinnaird, J.A. & Batchelor, R.A. (1987): Niger-Nigerian alkaline ring complexes: a classic example of African Phanerozoic anorogenic mid-plate magmatism. *In* Alkaline Igneous Rocks (J.G. Fitton & B.G.J. Upton, eds.). *Geol. Soc. London, Spec. Publ.* **30,** 357-379.

Brown, W.L. & Parsons, I. (1989): Alkali feldspars: ordering rates, phase transformations and behaviour diagrams for igneous rocks. *Mineral. Mag.* **53,** 25-42.

Cerling, T.E., Brown, F.H. & Bowman, J.R. (1985): Low-temperature alteration of volcanic glass: hydration, Na, K, ^{18}O and Ar mobility. *Chem. Geol. (Isotope Geosci. Sect.)* **52,** 281-293.

Condie, K.C. & Moore, J.M. (1977): Geochemistry of Proterozoic volcanic rocks from the Grenville Province, eastern Ontario. *In* Volcanic Regimes in Canada (W.R.A. Baragar, L.C. Coleman & J.M. Hall, eds.). *Geol. Assoc. Can., Spec. Pap.* **16,** 149-168.

Connelly, J.N., van Breemen, O. & Hanmer, S.K. (1987): The age of deformation related to the emplacement of the Elzevir Batholith and its regional implications, Grenville Province, southeastern Ontario. *Geol. Surv. Can., Pap.* **87-2,** 51-54.

Easton, R.M. (1989a): Project unit 88-05. Regional mapping and stratigraphic studies, Grenville Province. *Ontario Geol. Surv., Misc. Pap.* **146,** 153-157.

______ (1989b): Project unit 89-14. Regional alteration patterns and mineralization associated with the Deloro granite, Grenville Province, Madoc area. *Ontario Geol. Surv., Misc. Pap.* **146,** 158-168.

Hewitt, D.F. (1968): Geology of Madoc Township and the northern part of Huntingdon Township. *Ontario Dep. Mines, Geol. Rep.* **73.**

Jensen, L.S. (1976): A new cation plot for classifying subalkaline volcanic rocks. *Ontario Dep. Mines, Misc. Pap.* **66.**

Kretz, R. (1983): Symbols for rock-forming minerals. *Am. Mineral.* **68,** 277-279.

Kroll, H. & Ribbe, P.H. (1983): Lattice parameters, composition and Al-Si order in alkali feldspars. *In* Feldspar Mineralogy (P.H. Ribbe, ed.). *Rev. Mineral.* **2,** 57-99.

Le Bas, M.J., Le Maitre, R.W., Streckeisen, A. & Zanettin, B. (1986): A chemical classification of volcanic rocks based on the total alkali – silica diagram. *J. Petrol.* **27,** 745-750.

Lofgren, G.E. (1971): Experimentally produced devitrification textures in natural rhyolitic glass. *Geol. Soc. Am. Bull.* **82,** 111-124.

Malczak, J., Carter, T.R. & Springer, J.S. (1985): Base metal, molybdenum, and precious metal deposits of the Madoc – Sharbot Lake area, southeastern Ontario. *Ont. Geol. Surv., Open-File Rep.* **5548.**

Martin, R.F. (1984): Patterns of albitization in the Montgenèvre ophiolite, Western Alps. *Bull. Minéral.* **107,** 345-356.

Masuda, A., Nakamura, N. & Tanaka, T. (1973): Fine structure of mutually normalized rare-earth patterns of chondrites. *Geochim. Cosmochim. Acta* **37,** 239-248.

Miyashiro, A. (1978): Nature of alkalic volcanic rock series. *Contrib. Mineral. Petrol.* **66,** 91-104.

Moore, J.M., Jr. & Thompson, P.H. (1980): The Flinton Group: a late Precambrian metasedimentary succession in the Grenville Province of eastern Ontario. *Can. J. Earth Sci.* **17,** 1685-1707.

Orville, P.M. (1963): Alkali ion exchange between vapor and feldspar phases. *Am. J. Sci.* **261,** 201-237.

Payette, C. & Martin, R.F. (1986): The Harvey volcanic suite, New Brunswick. II. Postmagmatic adjustments in the mineralogy and bulk composition of a high-fluorine rhyolite. *Can. Mineral.* **24,** 571-584.

Pearce, J.A., Harris, N.B.W. & Tindle, A.G. (1984): Trace element discrimination diagrams for the tectonic interpretation of granitic rocks. *J. Petrol.* **25,** 956-983.

______ & Norry, M.J. (1979): Petrogenetic implications of Ti, Zr, Y, and Nb variations in volcanic rocks. *Contrib. Mineral. Petrol.* **69,** 33-47.

Sangster, A.L. & Bourne, J. (1982): Geology of the Grenville Province, and regional metallogenesis of the Grenville Supergroup. *In* Precambrian Sulphide Deposits, the H.S. Robinson Memorial Volume (R.W. Hutchinson, C.D. Spence & J.M. Franklin, eds.). *Geol. Assoc. Can., Spec. Pap.* **25,** 91-125.

SETHURAMAN, K. & MOORE, J.M., JR. (1973): Petrology of meta-volcanic rocks in the Bishop Corners – Donaldson area, Grenville Province, Ontario. *Can. J. Earth Sci.* **10**, 589-614.

SMITH, J.V. (1974): *Feldspar Minerals.* **1.** *Crystal Structure and Physical Properties.* Springer-Verlag, Berlin.

______ & BROWN, W.L. (1988): *Feldspar Minerals.* **1.** *Crystal Structures, Physical, Chemical, and Microtextural Properties* (Second ed.). Springer-Verlag, Berlin.

SMITH, R.L. & BAILEY, R.A. (1968): Resurgent cauldrons. *Geol. Soc. Am. Bull.* **113**, 613-662.

TAYLOR, S.R. & GORTON, M.P. (1977): Geochemical application of spark source mass spectrography. III. Element sensitivity, precision and accuracy. *Geochim. Cosmochim. Acta* **41**, 1375-1380.

THORNTON, C.P. & TUTTLE, O.F. (1960): Chemistry of igneous rocks. I. Differentiation index. *Am. J. Sci.* **258**, 664-684.

TUTTLE, O.F. (1952): Origin of the contrasting mineralogy of extrusive and plutonic salic rocks. *J. Geol.* **60**, 107-124.

______ & BOWEN, N.L. (1958): Origin of granite in the light of experimental studies in the system $NaAlSi_3O_8$ – $KAlSi_3O_8$ – SiO_2 – H_2O. *Geol. Soc. Am. Mem.* **74.**

VAN BREEMEN, O. & DAVIDSON, A. (1989): U–Pb zircon ages of granites and syenites in the Central Metasedimentary Belt, Grenville Province, Ontario. *Geol. Surv. Can., Pap.* **88-2**, 45-50.

VAN DE KAMP, P.C. (1968): Geochemistry and origin of meta-sediments in the Haliburton–Madoc area, southeastern Ontario. *Can. J. Earth Sci.* **5**, 1337-1372.

WU TSAI-WAY & KERRICH, R. (1986): Combined oxygen isotope – compositional studies of some granitoids from the Grenville Province of Ontario, Canada: implications for source regions. *Can. J. Earth Sci.* **23**, 1412-1432.

Received June 23, 1988, revised manuscript accepted for publication January 15, 1990.

APPENDIX 1: PETROGRAPHY OF SAMPLES

The rock types listed below are named in accordance with location in plot of total alkalis *versus* SiO_2 content (Fig. 2). Even though ion exchange has been significant in some samples, the total alkali content has not changed markedly. As a result, Figure 2 is still considered useful in defining rock types in this suite. The symbols used in the descriptions are those of Kretz (1983). No thin sections are available of M3, M16, F3, F23 and F24.

Relatively unmetasomatized mafic volcanic rocks

M1: trachyandesite, 5% phenocrysts of Pl embedded in a microcrystalline mosaic of anhedral feldspar + Qtz + chloritized Bt + opaque phases. Original amphibole now is replaced by Bt + Chl + opaque phases.
M4: trachyandesite, volcanic agglomerate, clasts of earlier trachytic material embedded in a cryptocrystalline groundmass interpreted to have been devitrified, then coarsened.
M7: andesite, no phenocrysts, aphyric rock, microcrystalline mosaic of feldspars + anhedral Bt + Qtz + Chl + opaque phases.
M18: dacite, no phenocrysts, microcrystalline mosaic of feldspars + Chl + Bt + Qtz; the feldspar laths are roughly aligned in a groundmass attributed an origin by flow; recrystallized, coarser-grained Bt–Chl bands formed along microfractures.
M19: trachyandesite, Bt–Chl bands and veins cross-cut a groundmass of broken Pl + Qtz + Kfs + Bt + Chl + opaque phases + Cal.

Na-metasomatized mafic volcanic rocks

M8: basalt, 30% phenocrysts of poikilitic prismatic actinolitic amphibole and rare large plagioclase crystals; microcrystalline groundmass of anhedral Ab + amphibole + opaque phases + Chl + minor Qtz.
M9: basalt, no phenocrysts, aphyric, similar to M8 but with microcrystalline bands alternating with coarser bands that contain amphibole prisms recrystallized perpendicular to primary banding, presumably along fluid pathways.
M11: trachyandesite, 10–15% phenocrysts of Pl and aggregates of poikilitic, anhedral Bt + Ms + opaque phases + Chl; microcrystalline groundmass of anhedral Ab + Bt + Qtz + opaque phases + Chl.
M12: trachyandesite, 15% phenocrysts, chessboard Ab, Ksp, recrystallized paramorphs after β-Qtz, with overgrowths, in a microcrystalline groundmass of Ab + Bt + Chl + opaque phases + Ep + Qtz + Ms. Subparallel microfractures (parallel to flow?) filled with Ms + Chl.
M13: trachyandesite, aphyric, trachytic texture, Ab laths with overgrowth, in a groundmass of anhedral feldspars + Bt + opaque phases + minor Cal. Alignment of laths attributed to flow.
M14: basalt, Pl, amphibole phenocrysts, amygdaloidal, recrystallized Ab laths + opaque phases + Chl + amphibole; amygdules filled with Cal + Ms + Qtz + Chl.
M15: basalt, 35% phenocrysts, poikilitic prisms of actinolitic amphibole, microcrystalline groundmass of Ab + Chl + anhedral amphibole + Chl + opaque phases + Qtz.

K-metasomatized mafic volcanic rocks

M6: tephrite, no primary phenocrysts; microphenocrysts of opaque phases set in a microcrystalline mosaic of chloritized Bt replaced by Ms, feldspar and Cal. Coarse secondary carbonate is common.

Relatively unmetasomatized felsic volcanic rocks

F4: "phonolite", volcanic agglomerate; clasts showing a trachytic texture are embedded in cryptocrystalline assemblage attributed to devitrification. Some clasts show Pl, Bt microphenocrysts and a "flood" of tiny anhedral opaque grains.

F8: trachyte, microporphyritic texture; large Pl laths define a trachytic texture in a cryptocrystalline feldspathic groundmass. Laths are very irregular owing to continued growth into groundmass. Secondary Cal + Ms.
F10: trachyte, 15% phenocrysts (glomeroporphyritic texture) of Pl + Kfs in a microcrystalline groundmass; mafic minerals are now opaque phases and Chl. Clasts of trachytic-textured material.
F11: trachyte, volcanic agglomerate, clasts of trachytic-textured material in a groundmass of microcrystalline feldspars + Qtz.

Na-metasomatized felsic volcanic rocks

F5: rhyolite, rare Ab phenocrysts in cryptocrystalline groundmass of Qtz + Ab + Ksp; rare Ms + Cal, rare spherulites. Groundmass is attributed to devitrification.
F5b: rhyolite, fragmented phenocrysts; cryptocrystalline groundmass shows spherulitic texture, interpreted to result by devitrification.
F5c: rhyolite, aphyric; cryptocrystalline groundmass of anhedral Qtz + Ab + secondary Ms + Cal; spherulitic texture.
F6: rhyolite, 10% phenocrysts of Ab (some broken) with irregular overgrowth into groundmass; glomeroporphyritic texture; microcrystalline spherulitic groundmass of Ab + Qtz.
F7: rhyolite, 15–20% phenocrysts, mostly Ab, some Qtz, glomeroporphyritic texture, microcrystalline groundmass of Ab + Qtz locally in a coarsened spherulitic texture; aggregates of cross-hatched Mc + minor Ms also present.
F9: rhyolite, 20% phenocrysts (glomeroporphyritic texture) of complexly twinned Ab + paramorphs after β-Qtz in a microcrystalline groundmass of anhedral Qtz + Ab + rare Ksp, with Ms + Chl + Cal. Phenocrysts overgrown into groundmass, and now have very irregular outline; groundmass attributed to devitrification.
F14: trachyte, no phenocrysts; trachytic texture defined by feldspar laths, attributed to flow. Cryptocrystalline mosaics of Ab + Qtz + opaque phases + Cal + Ms.
F16: trachydacite, no phenocrysts; trachytic-textured Ab laths set in a cryptocrystalline groundmass. Ms + Chl present.

K-metasomatized felsic volcanic rocks

F1: trachyte, 5–10% broken phenocrysts of Ksp (in part originally Pl?), irregular outline due to overgrowth into groundmass; cryptocrystalline groundmass of anhedral Ksp + opaque phases + Qtz + Ab + Bt + Ms. Groundmass attributed an origin by devitrification.
F2: trachyte; a largely fragmental rock containing clasts of trachytic-textured material in a devitrified groundmass. Secondary Ms.
F12: trachydacite, 5% feldspar phenocrysts (interpreted to have been plagioclase, now K-metasomatized) in cryptocrystalline groundmass of Ksp + Qtz + opaque phases + Ms + Ep. Groundmass attributed an origin by devitrification.
F13: rhyolite, 10% phenocrysts of Ksp + Pl (partly K-metasomatized), serrated rim due to overgrowth from groundmass, glomeroporphyritic texture, microcrystalline groundmass of anhedral Ksp + Qtz. Texture of matrix attributed to devitrification.
F15: rhyolite, relatively coarse-grained bands of Ksp + Qtz in cryptocrystalline bands of same composition. Cross-hatched Mc and Ms line microcavities. Seriate-textured groundmass attributed to devitrification.
F18: trachyte, 10% phenocrysts (broken) of Qtz and Ksp with serrated rims due to overgrowth from groundmass, in a microcrystalline groundmass of anhedral feldspars + Qtz + opaque phases + Bt. Groundmass attributed to devitrification.
F20: "phonolite", 5% phenocrysts of paramorphs after β-Qtz + Ksp (K-metasomatized Pl?), continued growth from groundmass, which contains feldspar laths and anhedral Qtz + Ksp. Irregular areas of fine cryptocrystalline greyish matrix along with microcrystalline material are present. Trachytic texture. Secondary Qtz + cross-hatched Mc. Main part of groundmass is attributed an origin by devitrification.